

MIT Open Access Articles

Monsoon circulations and tropical heterogeneous chlorine chemistry in the stratosphere

The MIT Faculty has made this article openly available. **Please share** how this access benefits you. Your story matters.

Citation: Solomon, Susan, Doug Kinnison, Rolando R. Garcia, Justin Bandoro, Michael Mills, Catherine Wilka, Ryan R. Neely, et al. "Monsoon Circulations and Tropical Heterogeneous Chlorine Chemistry in the Stratosphere." *Geophysical Research Letters* 43, no. 24 (December 27, 2016): 12,624–12,633.

As Published: <http://dx.doi.org/10.1002/2016GL071778>

Publisher: American Geophysical Union (AGU)

Persistent URL: <http://hdl.handle.net/1721.1/109491>

Version: Author's final manuscript: final author's manuscript post peer review, without publisher's formatting or copy editing

Terms of use: Creative Commons Attribution-Noncommercial-Share Alike



1
2
3
4
5
6
7
8
9
10
11
12
13
14
15
16
17
18
19
20
21
22
23
24
25

Monsoon circulations and

tropical heterogeneous chlorine chemistry in the stratosphere

Susan Solomon¹, Doug Kinnison², Rolando R. Garcia², Justin Bandoro¹, Michael Mills²,
Catherine Wilka¹, Ryan R. Neely III^{3,4}, Anja Schmidt³, John Barnes⁵, Jean-Paul
Vernier^{6,7}, Michael Höpfner⁸

¹Department of Earth, Atmospheric, and Planetary Sciences, Massachusetts Institute of Technology,
Cambridge, MA 02139

²Atmospheric Chemistry Observations and Modeling Laboratory, National Center for Atmospheric
Research, Boulder, CO 80307

³School of Earth and Environment, University of Leeds, Leeds, UK

⁴National Centre for Atmospheric Science, University of Leeds, Leeds, UK

⁵NOAA/Mauna Loa Observatory, Hilo, HI 96720

⁶NASA Langley Research Center, Hampton, VA

⁷Science Systems and Applications, Inc., Hampton, VA

⁸Institute of Meteorology and Climate Research, Karlsruhe Institute of Technology, Karlsruhe, Germany

Key Points.

- Transport linked to the monsoons brings increased HCl into contact with liquid aerosols in the cold tropical lowermost stratosphere.
- Model results indicate that monsoon flows lead to tropical activation of reactive chlorine on volcanic and non-volcanic particles.
- Heterogeneous chlorine activation contributes to the ozone budget and to tropical lowermost stratosphere ozone trends.

26 Abstract. Model simulations presented in this paper suggest that transport processes
27 associated with the summer monsoons bring increased abundances of hydrochloric acid
28 into contact with liquid sulfate aerosols in the cold tropical lowermost stratosphere,
29 leading to heterogeneous chemical activation of chlorine species. The calculations
30 indicate that the spatial and seasonal distributions of chlorine monoxide and chlorine
31 nitrate near the monsoon regions of the northern hemisphere tropical and subtropical
32 lowermost stratosphere could provide indicators of heterogeneous chlorine processing.
33 In the model, these processes impact the local ozone budget and decrease ozone
34 abundances, implying a chemical contribution to longer-term northern tropical ozone
35 profile changes at these altitudes.

36

37 1. Introduction

38

39 Heterogeneous chlorine chemistry on and in liquid polar stratospheric particles is thought
40 to play a significant role in polar and subpolar ozone depletion (Solomon et al., 1999
41 review, and references therein). Previous studies have not provided evidence for
42 heterogeneous chlorine chemistry occurring in the tropical stratosphere. Using the
43 current best understanding of liquid stratospheric particle chemistry in a state-of-the-art
44 numerical model, we examine whether such processes should be expected to affect
45 tropical composition, particularly at and slightly above the cold tropical tropopause, in
46 association with the Asian and North American summer (June-July-August) monsoons.
47 Further, we probe whether volcanic emissions of sulfur (which can increase stratospheric
48 sulfate aerosol abundances) could enhance this chemistry. The primary focus of this

49 paper is to examine whether ClO and ClONO₂ observations near the monsoon regions in
50 the tropical lowermost stratosphere could provide a novel testbed for understanding
51 stratospheric chlorine activation chemistry, while a secondary focus is on whether such
52 chemistry has the potential to contribute to the budget and trends of the tropical ozone
53 profile below about 20 km. Stratospheric chlorine chemistry has been a subject of
54 interest for decades, but key uncertainties remain in heterogeneous reactions rates (e.g.,
55 1-sigma uncertainties in reaction rates of 40%; JPL, 2011) that may be testable in new
56 ways in the tropics. The ozone profile trends in the tropical lowermost stratosphere have
57 long been a topic of scientific interest (Randel, 1999; Randel and Thompson, 2011) and
58 are thought to be largely dynamical in origin (e.g., WMO/UNEP 2014 and references
59 therein). Understanding whether there may be a potential chemical contribution to
60 tropical lower stratospheric ozone profile trends is hence of substantial scientific interest
61 and a secondary goal of this paper.

62

63 Monsoons are primarily driven by continental heating, extend into the lower stratosphere
64 (e.g., Dunkerton, 1995), and involve deep convection and formation of strong anti-
65 cyclonic circulation cells on a seasonal basis, maximizing in summer over Asia and North
66 America (e.g., Gettelman et al., 2004; Park et al., 2007; Randel et al., 2010). Weaker
67 monsoons are observed over southern hemisphere landmasses. Observations have shown
68 that transport related to the monsoons influences a range of chemicals in the tropical and
69 subtropical tropopause regions, including tracers such as carbon monoxide and hydrogen
70 cyanide (Randel et al., 2010), ozone (Park et al., 2007), volcanic and pollution aerosols
71 (Vernier et al., 2011; 2015) and water vapor (e.g., Rosenlof et al., 1997; Randel et al.,

72 2015; Schoeberl et al., 2013, Ploeger et al., 2013). Water vapor can play a role in
73 heterogeneous chemistry under cold conditions, both through its influence on formation
74 of ice clouds and through the dependence of chlorine activation reactions on the water
75 content of liquid stratospheric aerosol particles (which contain sulfuric acid and water,
76 see, e.g., Solomon, 1999; Thornton et al., 2007; Anderson et al., 2012). The influences
77 of HCl, water vapor, and temperature changes for stratospheric chlorine chemistry in the
78 tropics are discussed further below.

79

80 The primary goal of this paper is to probe the extent to which heterogeneous chlorine
81 chemistry may be expected to occur on liquid sulfate aerosols in the tropical stratosphere.
82 Liquid aerosol effects could represent a lower limit to this chemistry if, for example,
83 similar reactions also take place on tropical cirrus ice clouds, but the potential for ice
84 chemistry is not examined here. Heterogeneous halogen reactions on ice are sensitive to
85 the size distribution of cirrus ice particles (e.g., Bregman et al., 1997) and to the adopted
86 parameterization of cirrus clouds in models. Heterogeneous processing involving
87 chlorine, bromine, and iodine have also been identified on liquid and/or ice aerosols in
88 the troposphere (e.g., Wang et al., 2015; Schmidt et al., 2016; Saiz-Lopez and Fernandez,
89 2016; Von Hobe et al., 2011; see the review by Simpson et al., 2015 and references
90 therein) but the focus here is on stratospheric chlorine chemistry and the role of transport
91 via the monsoon circulations.

92 Recent progress in stratospheric chemistry modeling underpins this study. State-of-the-
93 art atmospheric chemistry models have been extensively intercompared and tested (e.g.,
94 Eyring et al., 2010), and the temperature-sensitive heterogeneous chemistry can be driven

95 by specified dynamics and temperatures from reanalysis fields based on observations;
96 here we use the Community Earth System Model, version 1, with the Whole Atmosphere
97 Community Climate Model version 4, as the atmospheric component
98 (CESM1(WACCM); see Marsh et al., 2013). The model's representation of
99 heterogeneous chemistry was shown to be in broad agreement with polar ozone and
100 constituent observations in Solomon et al. (2015), supporting its use to examine other
101 regions.

102 The stratospheric aerosol distributions employed in this model include representations of
103 both volcanic and non-volcanic sulfur sources. The calculated aerosol properties were
104 discussed in detail in Mills et al. (2016), and shown to compare well to total stratospheric
105 aerosol extinction data from lidars, including the Mauna Loa lidar. Further comparisons
106 to ground-based and satellite lidar backscatter data in the lowermost tropical stratosphere
107 are presented below. During the summer of 2011, tropical stratospheric aerosols were
108 enhanced compared to several other recent years, at least in part due to volcanic inputs
109 from the Nabro eruption in mid-June (Bourassa et al., 2012; Fairlie et al., 2013; Neely et
110 al., 2013) although pollution from Asian sources also contributes to aerosol loading in the
111 monsoon region (Vernier et al., 2015). In this paper we focus on 2011 as a period
112 when high tropical volcanic aerosol loading should be expected to increase the potential
113 role of the chemistry under consideration, and we compare 2011 to calculations for other
114 years.

115 2. Model Description

116

117 The specified dynamics version of CESM1 (WACCM), herein referred to as SD-

118 WACCM, is nudged to externally specified dynamical fields for temperature, zonal and
119 meridional winds, and surface pressure fields from the Modern Era Retrospective
120 Analysis for Research and Applications (MERRA; see Rienecker et al., 2011). The
121 procedure used to constrain the model is described by Marsh (2011) and Kunz et al.
122 (2011). The chemistry scheme includes the O_x , NO_x , HO_x , ClO_x , and BrO_x chemical
123 families, along with gas phase and heterogeneous reactions on liquid binary and ternary
124 sulfate aerosols. About 5 pptv of bromine from very-short lived substances (VSLS)
125 contributes to the modeled stratospheric bromine levels, along with CH_3Br and halon
126 sources. Chlorine from CH_3Cl , CH_3CCl_3 , and industrial chlorofluorocarbons is included
127 in the model. Arguably, our results represent a lower limit since chlorine from VSLS
128 may also contribute (see Hossaini et al, 2015) but are not included here, nor is convective
129 lofting of sea salt evaluated (e.g., Schmidt et al., 2016). Such additional sources of
130 chlorine and bromine could add to the chemical effects identified here if they reach the
131 stratosphere. Iodine chemistry is not included in the model; if there were to be iodine
132 input to the stratosphere akin to that identified in the upper troposphere, (see e.g.,
133 Volkamer et al., 2015; Saiz-Lopez and Fernandez, 2016) that could further affect the
134 chemistry of the region considered, but is not represented in this model. The
135 homogeneous and heterogeneous reactions and rate coefficients used in the simulations in
136 this paper are based on JPL (2011) except where indicated in Solomon et al. (2015).

137 We employ monthly averaged atmospheric aerosol distributions from Mills et al. (2016),
138 which were calculated using gas phase sulfur and related chemistry along with an aerosol
139 model in SD-WACCM. A database of volcanic SO_2 emissions and plume altitudes was
140 developed for eruptions between 1990 and 2014 by Neely and Schmidt (2016), and these

141 volcanic sulfur inputs along with background sources of sulfur (including OCS,
142 anthropogenic SO₂, etc.) were used to simulate stratospheric sulfate aerosols (Mills et al.,
143 2016). Aerosols are modeled as three lognormal modes: Aitken, accumulation, and
144 coarse. The model is capable of representing interactions of aerosol particles including
145 nucleation, condensation, coagulation, and sedimentation; for further details and
146 comparisons to observations, see Mills et al. (2016).

147 Three sets of SD-WACCM chemistry model results probe heterogeneous chlorine
148 chemistry in this paper: (i) simulations including volcanic and non-volcanic aerosol
149 sources; (ii) volcanically-clean simulations that include only background sources of
150 sulfur and (iii) simulations in which heterogeneous reactions are turned off between 40°N
151 and 40°S (but allowing heterogeneous reactions that do not involve chlorine or bromine
152 (e.g., N₂O₅+H₂O) to continue to occur).

153 3. Results

154

155 Figure 1 shows the distributions of calculated HCl obtained in SD-WACCM along with
156 the temperature distributions for the month of July, 2011 at 100 and 85 hPa, compared to
157 HCl observations for the channel centered at 100 hPa from the Microwave Limb Sounder
158 (MLS) instrument (Froidevaux et al., 2008), version 4.2. Model meteorological
159 tropopauses in the northern tropics at this time of year are from 90 to 130 hPa depending
160 upon longitude. No MLS data for HCl are available at 85 hPa, and the sounder has a
161 fairly broad vertical weighting function (see Figure 3 of Froidevaux et al., 2008). The
162 wind vectors superimposed in Figure 1 show the anti-cyclonic large-scale circulations
163 associated with the monsoonal flows over Asia and North America, and the temperatures

164 prescribed in SD-WACCM from MERRA are also overlaid in the bottom panel. While
165 temperatures near the tropopause in the summer monsoon regions are warmer than in
166 winter, they are nevertheless much colder than temperatures at mid-latitudes at these
167 altitudes, as can be seen in the overlaid contours of Figure 1.

168

169 The HCl gradients in the data and the model are qualitatively similar but display some
170 important quantitative differences. While the model tropical minima near 100 hPa are
171 lower than the MLS minima, a high bias of about 200 pptv at low to mid-latitudes in
172 MLS was noted in Froidevaux et al. (2008); further, tropical HCl by the infrared
173 HALogen Occultation Experiment (HALOE) are about 15% lower than MLS
174 (Froidevaux et al., 2005; see also Schoeberl et al., 2008). Froidevaux et al. (2008,
175 figures 11 and 14) also showed larger local differences of up to 20-50% at 100 hPa in
176 parts of the tropics in comparisons of MLS with HALOE and the Atmospheric Chemistry
177 Experiment (ACE). In all of these satellite data sources however, the HCl abundances
178 are much lower in the tropical lower stratosphere than in the extratropics; this is a robust
179 feature that is key to our analysis as discussed below.

180

181 Tropical regions are characterized on average by upwelling airmasses, in which chlorine
182 is largely expected to be tied up in unreactive organic chlorine source gases (mainly
183 CH₃Cl and chlorofluorocarbons). When these gases travel upward and poleward in the
184 stratosphere, their chemical breakdown supplies inorganic chlorine. The inorganic
185 chlorine can interact with sufficiently cold and wet surfaces and activate the chlorine. In
186 the two polar regions, this chemistry enhances ClO and destroys ozone. Chlorine

187 activation and related chlorine-catalyzed ozone loss has been documented following its
188 discovery in association with the Antarctic ozone hole, but it has been generally assumed
189 that similar chemistry was negligible in the tropics due to insufficient inorganic chlorine
190 (see, e.g., Solomon, 1999 for a review stating this assertion). However, Figure 1 shows
191 that, in our model, the monsoon circulations lead to equatorward transport of inorganic
192 chlorine into the northern subtropics and tropics along the eastern side of the monsoon
193 anticyclones, and the MLS data supports these general features. Recent studies have
194 emphasized the importance of quasi-horizontal transport in producing larger abundances
195 of several key chemical constituents (including ozone and HCl) in the northern tropics as
196 compared to the southern tropics (e.g., Konopka et al., 2010; Ploeger et al., 2012; Abalos
197 et al., 2012; Stolarski et al., 2014).

198

199 Figure 1 highlights the role of equatorward transport of extratropical air on the eastern
200 flanks of the northern hemisphere monsoon anticyclones, substantially increasing
201 available inorganic chlorine at northern subtropical latitudes in summer in this model and
202 in the observations. The combination of relatively cold temperatures, liquid aerosols, and
203 transport of inorganic chlorine from higher latitudes drives low-latitude heterogeneous
204 chlorine activation and enhances calculated ClO in our model. Figure 2 presents maps
205 of ClO and ClONO₂ calculated in the model at 17 km for July 2011 when low-latitude
206 heterogeneous chlorine chemistry is included. Supplemental figure S1 shows the
207 distributions of the rates of chemical processes that serve to activate chlorine, and Table
208 S1 indicates sensitivities of the key activation reaction rate constant to the range of
209 temperature and water vapor changes in the regions of maximum activation, illustrating

210 that the temperature changes are much more important than the water vapor changes for
211 enhancing the chemical reactivity. The largest heterogeneous chlorine activation rates
212 occur near 15-20°N, particularly where the southward flow around the Asian monsoon
213 brings high levels of inorganic chlorine into the coldest part of the subtropical lower
214 stratosphere, where the eastern edge of the anticyclone flows into the Western Pacific.
215 Temperatures as cold as 194-196K are found even in summer near, for example, 135°E in
216 this region (Figures 1, 2, and S1).

217

218 Local maxima in ClO of over 30 pptv (monthly mean) are calculated near the Asian
219 monsoon region near 17 km, while peak values of 15 pptv are obtained near the North
220 American monsoon region (Figure 2). Chlorine activation can be expected to produce
221 enhanced ClONO₂ downwind of the main activation region, provided that NO_x is not
222 completely removed by the heterogeneous processing. This chemistry forms the well-
223 known ClONO₂ ‘collar’ at sub-polar latitudes (e.g., Toon et al., 1989). Figure 2 shows
224 that the model calculates ClONO₂ values as large as 50-75 pptv near the ClO maxima,
225 linked to the North American and Asian summer monsoons. The calculated tropical
226 stratospheric chlorine activation depicted in Figure 2 has not been discussed in previous
227 studies of which we are aware.

228

229 A consequence of elevated ClO concentrations is potential destruction of stratospheric
230 ozone. When the tropical heterogeneous chlorine chemistry identified here is included
231 compared to calculations excluding it, we calculate ozone decreases (averaged over the
232 years 2009-2012 and over the northern tropics from 0-30°N) of about 2.5% at 16-17 km,

233 about 1.5% at 18 km, and about 1% at 19 km. For comparison, the estimated tropical
234 average ozone trends are about 1-4% per decade from 17-19 km over 1980-2005 (Randel
235 and Thompson, 2011; their figure 12).

236

237 The catalytic cycle involving chlorine and hydrogen radicals (in which the rate limiting
238 step is $\text{ClO} + \text{HO}_2$) dominates our calculated ozone decreases, but the inter-halogen
239 reaction between ClO and BrO also represents about 25% of the modeled ozone decrease.
240 These numbers imply an effect on the local ozone budget due to heterogeneous chlorine
241 chemistry, and whether this change represents anthropogenic ozone depletion (as
242 opposed to a change in the ozone background state) depends upon the balance between
243 chlorine and bromine from industrial chemicals versus natural sources in this region,
244 particularly very short-lived species (VSLS) with biogenic origins. In our model, the
245 balance between industrial and VSLS sources of chlorine and bromine suggests that
246 about three-quarters of the calculated ozone change is traceable to anthropogenic
247 emissions. While it remains likely that most of the ozone trend in tropical lower
248 stratosphere ozone since 1979 is linked to dynamical changes (Randel and Thompson,
249 2011), our work implies that heterogeneous chlorine chemistry may have made some
250 contributions to the vertical profile of trends in ozone in this region. The changes are
251 confined to a narrow height range, and the corresponding decreases in column ozone for
252 calculations including heterogeneous chemistry to those without them at, for example,
253 15N in summer, vary between 1-2DU over 2009-2011. More detailed analysis of
254 tropical ozone trends is outside the scope of the present paper.

255

256 Figure 3 presents the zonally averaged distributions of ClONO₂ versus latitude and
257 altitude for July, 2011 for these SD-WACCM simulations. The location of the
258 meteorological tropopause is indicated in the figure. When low latitude heterogeneous
259 chlorine chemistry is included in the model, the calculated stratospheric gradient in
260 ClONO₂ from about 16-18 km and from about 10-25N in July 2011 displays a
261 pronounced ‘tongue’, with peak zonal mean abundances of over 40 pptv, while no such
262 tongue is obtained in the model without heterogeneous chemistry. Figure 3 illustrates
263 that the region substantially affected by the chemistry considered here is confined to a
264 limited range of height and latitude.

265

266 Figure 4 presents seasonal changes in ClO and ClONO₂ over several years at 17 km
267 averaged over the latitude band from 14-20°N for the three model test cases noted above:
268 with volcanic sulfur inputs, for volcanically clean conditions, and with the heterogeneous
269 chlorine activation chemistry turned off. Figure 4 shows that the calculated
270 heterogeneous chemical processes greatly increase the modeled concentrations of ClO
271 and ClONO₂ compared to calculations without heterogeneous chemistry. The changes in
272 these two species as compared to the no heterogeneous chemistry case exceed their
273 interannual variability, and are robust to substantial seasonal changes in HCl from month
274 to month (i.e., June-July-August) or interannually (see Figures 4 and S2). Considerably
275 smaller relative changes that lie within interannual variations are expected for HCl
276 (Figure S2). Figure 4 also presents averaged measured satellite extinction in the
277 monsoon region (15-45°N, 5-105°E) at 15, 16, and 17 km (adapted from Figure 2 in
278 Vernier et al., 2015) as compared to the model. As a further check on the modeled

279 aerosols over broader parts of the tropics, Figure 4 compares observations of lidar
280 backscatter from Mauna Loa observatory (19°N) integrated from 15-20 km to that from
281 the model at the same site; the modeled extinction has been converted to backscatter here
282 using a backscatter to extinction conversion factor of 40 (note different y-axes for model
283 and data in the bottom panel of Figure 4). Jaeger and Hofmann (2002, 2003) suggest
284 values of about 20-60 for this conversion factor depending on particle sizes, with lower
285 values for larger particles following major eruptions. Figure 4 shows that the model
286 captures the timing and magnitudes of the volcanic enhancements that are apparent in
287 both sets of observations. The modeled absolute values are generally close to the Vernier
288 et al. (2015) data but are somewhat lower than the Mauna Loa data.

289

290 The calculated chlorine activation that is evident in Figure 4 varies from year to year and
291 month to month depending on multiple factors: the strength of the transport associated
292 with the monsoons (which affects total chlorine), changes in temperature, and changes in
293 stratospheric aerosol amounts (see Fig. S1). It is likely that the quasi-biennial oscillation
294 plays a role in modulating transport of HCl from year to year (Schoeberl et al., 2008), and
295 the El Niño is also important for temperature variations, particularly in the warm pool
296 region of maximum activation (e.g., Rosenlof and Reid, 2008; Nishimoto and Shiotani,
297 2012).

298

299 The model results shown in Figure 4 suggest that heterogeneous chlorine chemistry in
300 this region greatly enhances reactive chlorine species even for volcanically clean
301 conditions, with substantial increases above what would be expected without

302 heterogeneous processing. Figure 4 suggests summer ClO and ClONO₂ abundances in
303 this region when heterogeneous chlorine reactions are simulated for non-volcanic
304 conditions are of the order of 5 and 25-40 pptv respectively, compared to only a few
305 tenths of a pptv and 5-10 pptv when these reactions are neglected. Further increases of
306 the order of 10 pptv for ClO and 5-8 pptv for ClONO₂ are simulated in volcanically
307 perturbed summers, particularly 2011 (after Nabro) and 2009 (when transport of aerosol
308 to the tropics from the Sarychev eruption has been documented; see Figure 1 in Solomon
309 et al., 2011).

310

311 4. Discussion and Conclusions

312

313 Heterogeneous chlorine chemistry has been well established in polar regions through
314 extensive measurements and modeling, and it should be expected to operate in other
315 latitudes if conditions allow. In this paper, we have shown that numerical model
316 simulations indicate that the appropriate conditions occur in association with the northern
317 hemisphere summer monsoons based on current chemical understanding.

318

319 Figures 1 and 2 taken together illustrate how the input of inorganic chlorine from mid-
320 latitudes and the relatively cold conditions of the tropical lowermost stratosphere region
321 combine to produce a rapid rate of chlorine activation on liquid sulfate aerosols near the
322 northern monsoon regions in SD-WACCM. The largest rates of calculated chlorine
323 activation are associated with flow around the Asian monsoon into the especially cold
324 lower stratosphere near the Western Pacific warm pool. Our model results suggest that

325 heterogeneous chlorine activation should greatly increase average ClO and ClONO₂
326 abundances from about 10-20N in the altitude range from 16-18 km as compared to
327 simulations neglecting this chemistry. Volcanic increases in liquid sulfate aerosols
328 enhance the perturbations, but the heterogeneous reactions are thought to be sufficiently
329 rapid that substantial changes are also indicated for volcanically clean conditions.
330
331 Many stratospheric chlorine chemistry measurements have focused on polar and subpolar
332 regions. We are not aware of any available datasets that have validated measurements of
333 ClO or ClONO₂ in the 16-18 km region of the tropics and subtropics against which our
334 findings could be further tested. Stratospheric chemistry is tightly coupled, and other
335 constituents including HCl, NO, NO₂, HOCl, etc. may also be useful to probe the impacts
336 of this heterogeneous chemistry. Laboratory studies of these reactions have used
337 H₂SO₄/H₂O and H₂SO₄/H₂O/HNO₃ solutions, and those studies form the basis for the
338 chemistry recommended in JPL (2011) and imposed in models. Even for pure
339 H₂SO₄/H₂O solutions, uncertainties in liquid heterogeneous reactivities are poorly
340 quantified, especially for temperatures below about 200K. Further, direct measurements
341 of particle composition in the tropical tropopause region have revealed substantial
342 amounts of other components, such as non-volatile species and pollutants including
343 organic compounds (Murphy, 2009; 2014; Borrmann et al., 2010). Whether these
344 components could alter the stratospheric liquid aerosol reactivity is unknown. If so, then
345 particle reactivities might differ in volcanic versus non-volcanic years, since the volcanic
346 particles would contain a much larger fraction of sulfuric acid, and hence provide a closer
347 correspondence to the laboratory data compared to non-volcanic conditions. Our

348 simulations provide a testable framework for examining whether or not heterogeneous
349 chlorine chemistry takes place in the tropical lowermost stratosphere, either under
350 volcanically clean or volcanically perturbed conditions, or both.

351

352 Acknowledgments and Data. We thank Dan Murphy and Brian Toon for helpful
353 discussions. SS and JB acknowledge funding under NSF-1539972 and NSF-1419667.

354 RN is supported by the Natural Environment Research Council (NERC) through the
355 National Centre for Atmospheric Science (NCAS) in the UK. AS was supported by an

356 Academic Research Fellowship from the University of Leeds and a NCAR visiting
357 researcher grant. JB is funded by NOAA/ESRL/GMD. The National Center for

358 Atmospheric Research (NCAR) is sponsored by the U.S. National Science Foundation.

359 Any opinions, findings, and conclusions or recommendations expressed in the publication
360 are those of the author(s) and do not necessarily reflect the views of the National Science

361 Foundation. WACCM is a component of the Community Earth System Model (CESM),
362 which is supported by the National Science Foundation (NSF) and the Office of Science

363 of the U.S. Department of Energy. Computing resources were provided by NCAR's

364 Climate Simulation Laboratory, sponsored by NSF and other agencies. This research was

365 enabled by the computational and storage resources of NCAR's Computational and

366 Information System Laboratory (CISL). We thank NASA Goddard Space Flight Center

367 for the MERRA data (accessed freely online at <http://disc.sci.gsfc.nasa.gov/>) and the

368 Aura MLS team for HCl data (accessed freely online at

369 <http://disc.sci.gsfc.nasa.gov/Aura/data-holdings/MLS>). Mauna Loa lidar data shown in

370 this paper may be accessed at <http://ndacc-lidar.org/>. Model results shown in this paper

371 are available on request to the WACCM liaison, Michael Mills mmills@ucar.edu.

372 References

373 Abalos, M., W. J. Randel, and E. Serrano (2012), Variability in upwelling across the
374 tropical tropopause and correlations with tracers in the lower stratosphere, *Atmos.*
375 *Chem. Phys.*, 12, 11,505–11,517, doi:10.5194/acp-12-11505-2012.

376 Anderson, J. G., Wilmouth, D. M., Smith, J. B., and D. S. Sayres (2012), UV dosage
377 levels in summer: Increased risk of ozone loss from convectively injected water
378 vapor, *Science*, 337, 835-839, doi: 10.1126/science.1222978.

379 Borrmann, S., et al. (2010), Aerosols in the tropical and subtropical UT/LS: in-situ
380 measurements of submicron particle abundance and volatility, *Atmos. Chem.*
381 *Phys.*, 10, 5573–5592, doi:10.5194/acp-10-5573-2010.

382 Bourassa, A. E., Robock, A., Randel, W. J., Deshler, T., Rieger, L. A., Lloyd, N. D.,
383 Llewellyn, E. J., and D. A. Degenstein (2012), Large volcanic aerosol load in the
384 stratosphere linked to Asian monsoon transport, *Science*, 337, 78-81,
385 doi:10.1126/science.1219371, 2012.

386 Bregman, A., M. van den Broek, K. S. Carslaw, R. Mueller, T. Peter, M. P. Scheele, and
387 J. Lelieveld, (1997), Ozone depletion in the late winter lower Arctic stratosphere:
388 Observations and model results, *J. Geophys. Res.*, 102, 10815-10828.

389 Dunkerton, T. J., (1995) Evidence of meridional motion in the summer lower stratosphere
390 adjacent to monsoon regions, *J. Geophys. Res.*, 100(D8), 16675–16688,
391 doi:10.1029/95JD01263.

392 Eyring, V., T. G. Sheperd, and D. W. Waugh (Eds.) (2010), SPARC report on the evalua-

393 tion of chemistry-climate models, SPARC Rep. No. 5, WRCP-132, WMO-TD
394 No. 1526, World Met. Org., Geneva.

395 Fairlie, T. D., J.-P. Vernier, M. Natarajan, and K. M. Bedka, (2014), Dispersion of the
396 Nabro volcanic plume and its relation to the Asian summer monsoon, *Atm. Chem.*
397 *Phys.*, 14, 7045-7057, doi:10.5194/acp-14-7045-2014.

398 Froidevaux, L., et al. (2008), Validation of Aura Microwave Limb Sounder HCl
399 measurements, *J. Geophys. Res.*, 113, D15S25, doi:10.1029/2007JD009025.

400 Gettelman, A., D. E. Kinnison, T. J. Dunkerton, and G. P. Brasseur (2004), Impact of
401 monsoon circulations on the upper troposphere and lower stratosphere, *J.*
402 *Geophys. Res.*, 109, D22101, doi:10.1029/2004JD004878.

403 Hossaini, R., M. P. Chipperfield, S. A. Montzka, A. Rap, S. Dhomse, and W. Feng,
404 (2015), Efficiency of short-lived halogens at influencing climate through
405 depletion of stratospheric ozone, *Nat. Geosci.*, 8, 186-190.

406 Jäger, H. and T. Deshler: Lidar backscatter to extinction, mass and area conversions for
407 stratospheric aerosols based on midlatitude balloonborne size distribution
408 measurements, *Geophys. Res. Lett.*, 29(19), 1929, doi:10.1029/2002GL015609,
409 2002. (correction *Geophys. Res. Lett.*, 30(7), 1382, doi:10.1029/2003GL017189,
410 2003).

411 Jet Propulsion Laboratory JPL (2011), Chemical kinetics and photochemical data for use
412 in atmospheric studies, evaluation number 15, JPL Publication, 06-2.

413 Konopka, P., J.-U. Grooß, F. Ploeger, and R. Müller (2009), R.: Annual cycle of
414 horizontal in-mixing into the lower tropical stratosphere, *J. Geophys. Res.*, 114,
415 D19111, doi:10.1029/2009JD011955.

416 Kunz, A., L. L. Pan, P. Konopka, D. E. Kinnison, and S. Tilmes, 2011: Chemical and
417 dynamical discontinuity at the extratropical tropopause based on START08 and
418 WACCM analyses. *J. Geophys. Res.*, 116, D24302, doi:10.1029/2011JD016686.

419 Marsh, D. R., 2011: Chemical-dynamical coupling in the mesosphere and lower
420 thermosphere, in *Aeronomy of the Earth's Atmosphere and Ionosphere, IAGA*
421 *Spec. Sopron Book Ser., Vol. 2*, edited by M. Abdu, D. Pancheva, and A.
422 Bhattacharyya, pp. 3–17, Springer, Dordrecht, Netherlands.

423 Marsh, D. R. M.J. Mills, D. E. Kinnison, J. F. Lamarque, N. Calvo, and L. M. Polvani,
424 (2013), Climate Change from 1850 to 2005 Simulated in CESM1(WACCM). *J.*
425 *Clim.*, 26, 7372–7391, doi: [10.1175/JCLI-D-12-00558.1](https://doi.org/10.1175/JCLI-D-12-00558.1)

426 Mills, M. J., et al. (2016), Global volcanic aerosol properties derived from emissions,
427 1990–2014, using CESM1(WACCM), *J. Geophys. Res.*, 121, 2332–2348,
428 doi:10.1002/2015JD024290.

429 Murphy, D. M., Thomson, D. S., and M. J. Mahoney (1998), *In situ* measurements of
430 organics, meteoric material, mercury, and other elements in aerosols at 5 to 19 km,
431 *Science*, 282, 1664–1669.

432 Murphy, D. M., Froyd, K. D., Schwarz, J. P., and J. C. Wilson (2014), Observations of
433 the chemical composition of stratospheric aerosol particles, *Q. J. Roy. Met. Soc.*,
434 140, 1269–1278.

435 Neely III, R.R., O.B. Toon, S. Solomon, J.-P. Vernier, C. Alvarez, J.M. English, K.H.
436 Rosenlof, M.J. Mills, C.G. Bardeen, J.S. Daniel and J.P. Thayer (2013), Recent
437 anthropogenic increases in SO₂ from Asia have minimal impact on stratospheric
438 aerosol, *Geophys. Res. Lett.*, 40, doi:10.1002/grl.50263.

439 Neely III, R.R. and A. Schmidt (2016), VolcanEESM (Volcanic Emissions for Earth
440 System Models): Volcanic sulphur dioxide (SO₂) emissions database from 1850
441 to present. Centre for Environmental Data Analysis, (2016).
442 <http://catalogue.ceda.ac.uk/uuid/bfbd5ec825fa422f9a858b14ae7b2a0d>.

443 Nishimoto, E., and M. Shiotani (2012), Seasonal and interannual variability in the
444 temperature structure around the tropical tropopause and its relationship with
445 convective activities, *J. Geophys. Res.*, 117, D02104,
446 doi:10.1029/2011JD016936.

447 Park, M., Randel, W. J., Gettelman, A., Massie, S. T., and J. H. Jiang, (2007), Transport
448 above the Asian summer monsoon anticyclone inferred from Aura Microwave
449 Limb Sounder tracers, *J. Geophys. Res.*, 112, D16309,
450 doi:10.1029/2006JD008294.

451 Ploeger, F., et al. (2013), Horizontal water vapor transport in the lower stratosphere from
452 subtropics to high latitudes during boreal summer, *J. Geophys. Res.*, 118, 8111–
453 8127, doi:10.1002/jgrd.50636.

454 Randel, W. J., R. S. Stolarski, D. M. Cunnold, J. A. Logan, M. J. Newchurch, and J. M.
455 Zawodny (1999), Trends in the vertical distribution of ozone, *Science*, 285, 1689–
456 1692.

457 Randel, W. J., et al. (2010), Asian monsoon transport of pollution to the stratosphere,
458 *Science*, 328, 611-613.

459 Randel, W. J., and A. M. Thompson, (2011), Interannual variability and trends in tropical
460 ozone derived from SAGE II satellite data and SHADOZ ozonesondes, *J.*
461 *Geophys. Res.*, 116, D07303, doi:10.1029/2010JD015195.

462 Randel, W. J., K. Zhang, and R. Fu (2015), What controls stratospheric water vapor in
463 the NH summer monsoon regions?, *J. Geophys. Res.*, 120, 7988–8001,
464 doi:10.1002/2015JD023622.

465 Rienecker, M. M., et al. (2011), MERRA: NASA’s Modern-Era Retrospective Analysis
466 for Research and Applications, *J. Clim.*, 24, 3624–3648, doi: 10.1175/JCLI-D-11-
467 00015.1.

468 Rosenlof, K. H., and G. C. Reid, (2008), Trends in the temperature and water vapor
469 content of the tropical lower stratosphere: Sea surface connection, *J. Geophys.*
470 *Res.*, 113, D06107, doi:10.1029/2007JD009109.

471 Rosenlof, K. H., A. F. Tuck, K. K. Kelly, J. M. Russell III, and M. P. McCormick (1997),
472 Hemispheric asymmetries in water vapor and inferences about transport in the
473 lower stratosphere, *J. Geophys. Res.*, 102, 13,213–13,234,
474 doi:10.1029/97JD00873.

475 Saiz-Lopez, A., and R. P. Fernandez, (2016), On the formation of tropical rings of atomic
476 halogens: causes and implications, *Geophys. Res. Lett.*, 43, 2928–2935,
477 doi:10.1002/2015GL067608.

478 Schoeberl, M. R., A. E. Dessler, and T. Wang (2013), Modeling upper tropospheric and
479 lower stratospheric water vapor anomalies, *Atmos. Chem. Phys.*, 13, 7783–7793,
480 doi:10.5194/acp-13-7783-2013.

481 Schoeberl, M. R., et al. (2008), QBO and annual cycle variations in tropical lower
482 stratosphere trace gases from HALOE and Aura MLS observations, *J. Geophys.*
483 *Res.*, 113, D05301, doi:10.1029/2007JD008678.

484 Schmidt, J. A., et al. (2016), Modeling the observed tropospheric BrO background:
485 Importance of multiphase chemistry and implications for ozone, OH, and mercury,
486 *J. Geophys. Res. Atmos.*, 121, doi:10.1002/2015JD024229.

487 Simpson, W. R., S. S. Brown, A. Saiz-Lopez, J. A. Thornton, and R. von Glasow (2015),
488 Tropospheric halogen chemistry: sources, cycling, and impacts, *Chem. Rev.*, 115,
489 4035–4062.

490 Solomon, S. (1999), Stratospheric ozone depletion, A review of concepts and history,
491 *Rev. Geophys.*, 37, 275–316.

492 Solomon, S., Daniel, J. S., Neely, R. R., Vernier, J.-P., Dutton, E. G. and W. L.
493 Thomason, (2011), The persistently variable “background” stratospheric aerosol
494 layer and global climate change, *Science*, 333(6044), 866–870,
495 doi:10.1126/science.1206027.

496 Solomon, S. D. Kinnison, J. Bandoro, and R. R. Garcia, (2015), Polar ozone depletion:
497 An update, *J. Geophys. Res.* 120, doi:10.1002/2015JD023365.

498 Stolarski, R. S., D. W. Waugh, L. Wang, L. D. Oman, A. R. Douglass, and P. A.
499 Newman (2014), Seasonal variation of ozone in the tropical lower stratosphere:
500 Southern tropics are different from northern tropics, *J. Geophys. Res.*, 119,
501 doi:10.1002/2013JD021294.

502 Thornton, B. F., Toohey, D. W., Tuck, A. F., Elkins, J. W., Kelly, K. K., Hovde, S. J.,
503 Richard E. C., Rosenlof, K. H., Thompson, T. L., Mahoney, M. J., Wilson, J. C.,
504 (2007) Chlorine activation near the midlatitude tropopause, *J. Geophys. Res.*, 112,
505 D18306, doi:10.1029/2006JD007640.

506 Toon, G. C., C. B. Farmer, L. L. Lowes, P. W. Schaper, J.-F. Blavier, and R. H. Norton
507 (1989), Infrared Aircraft Measurements of Stratospheric Composition Over
508 Antarctica During September 1987, *J. Geophys. Res.*, 94, 16,571–16,596, doi:
509 10.1029/JD094iD14p16571.

510 Vernier, J.-P., L. W. Thomason, and J. Kar (2011), CALIPSO detection of an Asian
511 tropopause aerosol layer, *Geophys. Res. Lett.*, 38, L07804,
512 doi:10.1029/2010GL046614.

513 Vernier, J.-P., T. D. Fairlie, M. Natarajan, F. G. Wienhold, J. Bian, B. G. Martinsson, S.
514 Crumeyrolle, L. W. Thomason, and K. M. Bedka (2015), Increase in upper
515 tropospheric and lower stratospheric aerosol levels and its potential connection
516 with Asian pollution, *J. Geophys. Res.*, 120, 1608–1619,
517 doi:10.1002/2014JD022372.

518 Volkamer, R., et al. (2015), Aircraft measurements of BrO, IO, glyoxal, NO₂, H₂O, O₂-
519 O₂, and aerosol extinction profiles in the tropics: comparison with aircraft- and

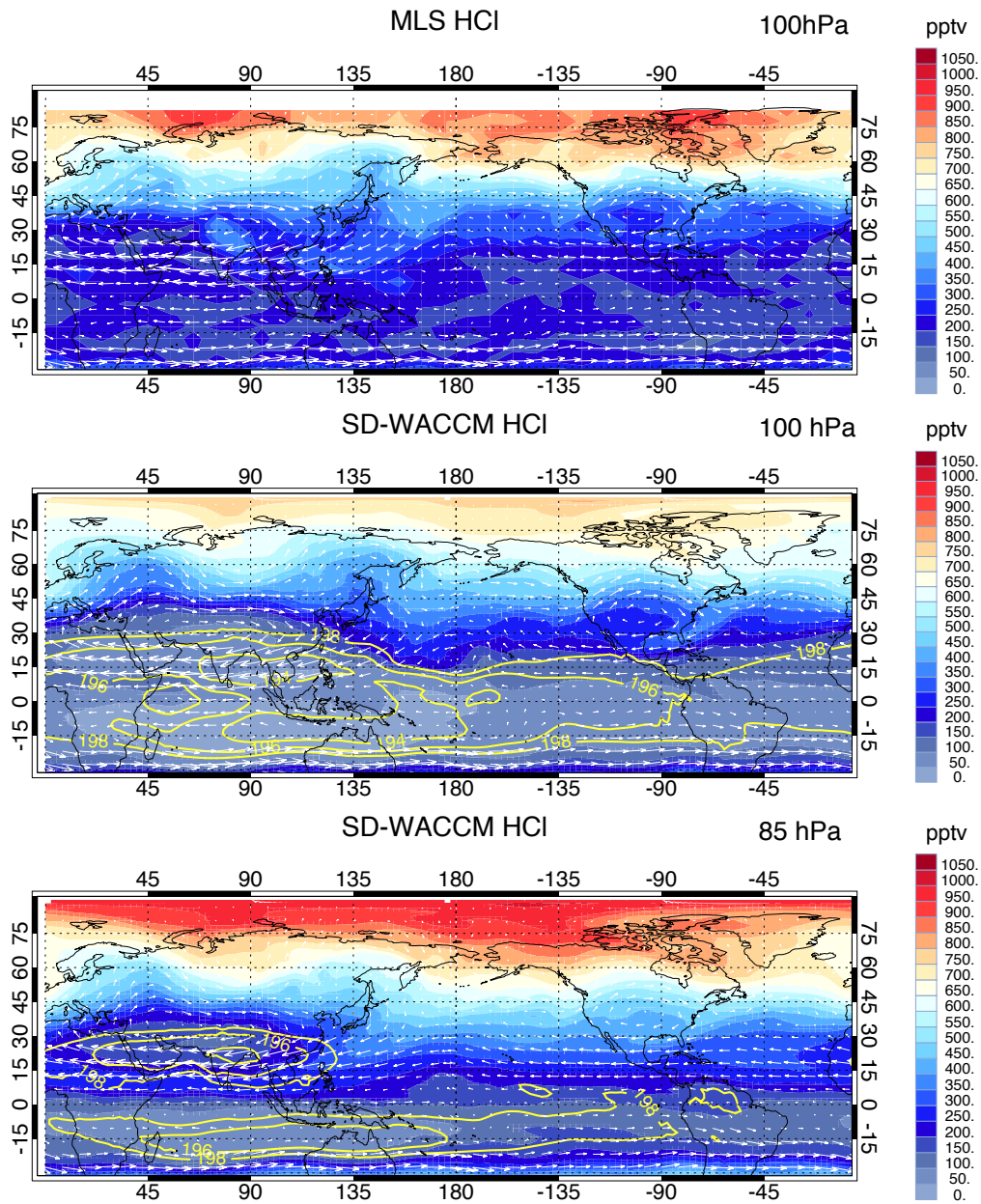
520 ship-based in situ and lidar measurements, *Atm. Meas. Tech.*, 8, 2121-2148.

521 Von Hobe, M. et al. (2011), Evidence for heterogeneous chlorine activation in the
522 tropical UTLS, *Atm. Chem. Phys.*, 11, 241-256, doi:10.5194/acp-11-241-2011.

523 Wang, S., et al. (2015), Active and widespread halogen chemistry in the tropical and
524 subtropical free troposphere, *Proc. Nat. Acad. Sci.*, 112, 9281-9286.

525 WMO/UNEP (2014), *Scientific assessment of ozone depletion: 2014*, World
526 Meteorological Organization Global Ozone Research and Monitoring Project,
527 Report 55, Geneva, Switzerland.

528

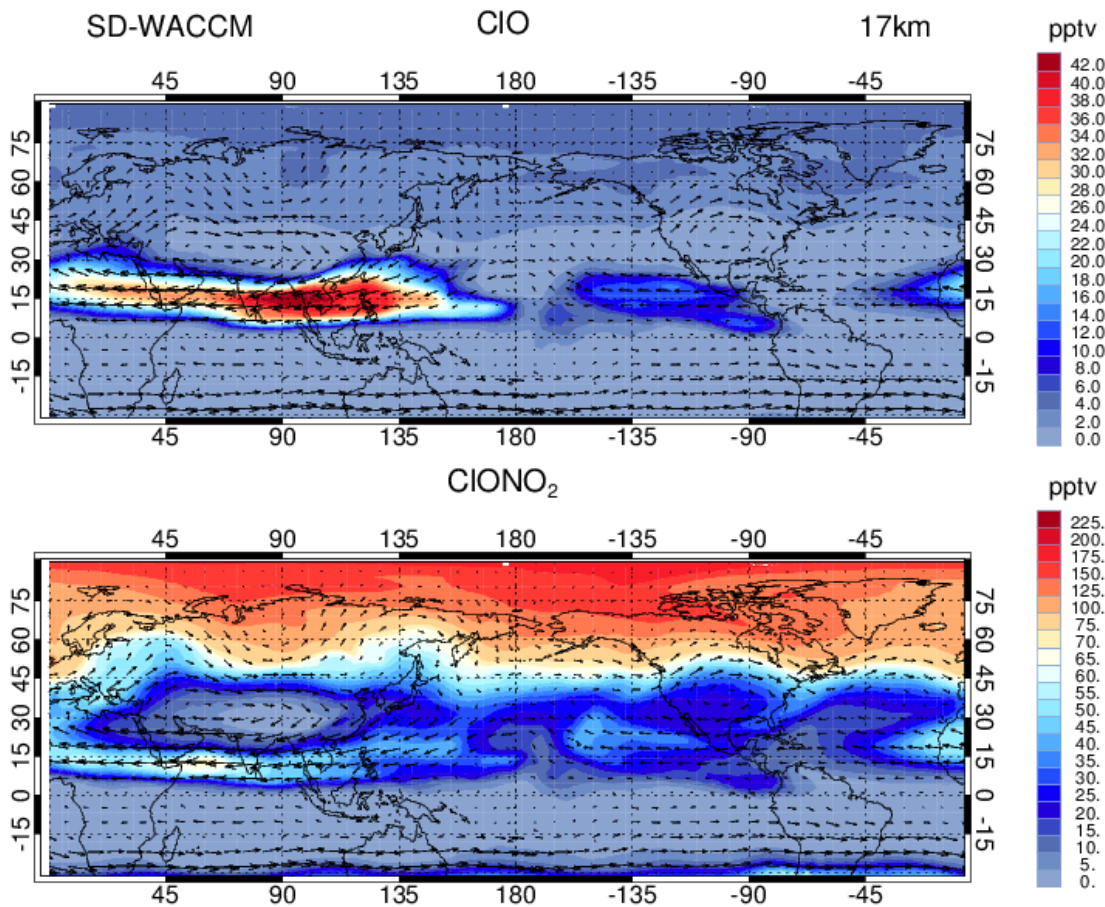


529

530 Figure 1. Distributions of HCl from MLS satellite data for the channel centered at 100

531 hPa (top) and at 100 and 85 hPa in SD-WACCM simulations for July 2011. Wind

532 vectors and temperatures from SD-WACCM are superimposed.



533

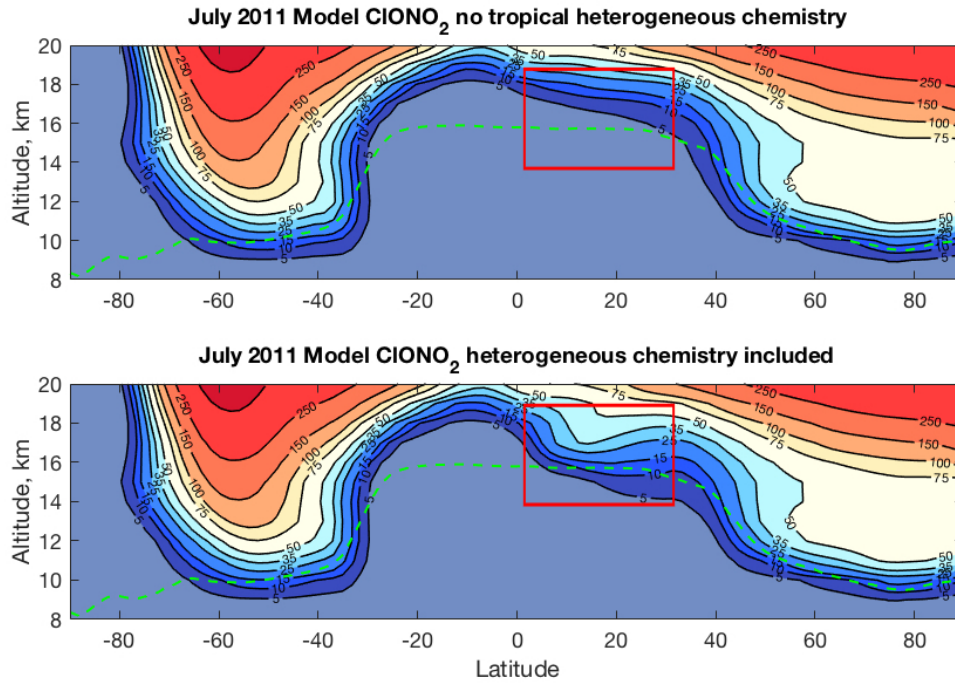
534

535 Figure 2. Model calculated monthly mean distributions of CIO (pptv, top panel),

536 ClONO₂ (pptv, bottom panel) for July 2011 at 17 km, with superimposed wind vectors.

537

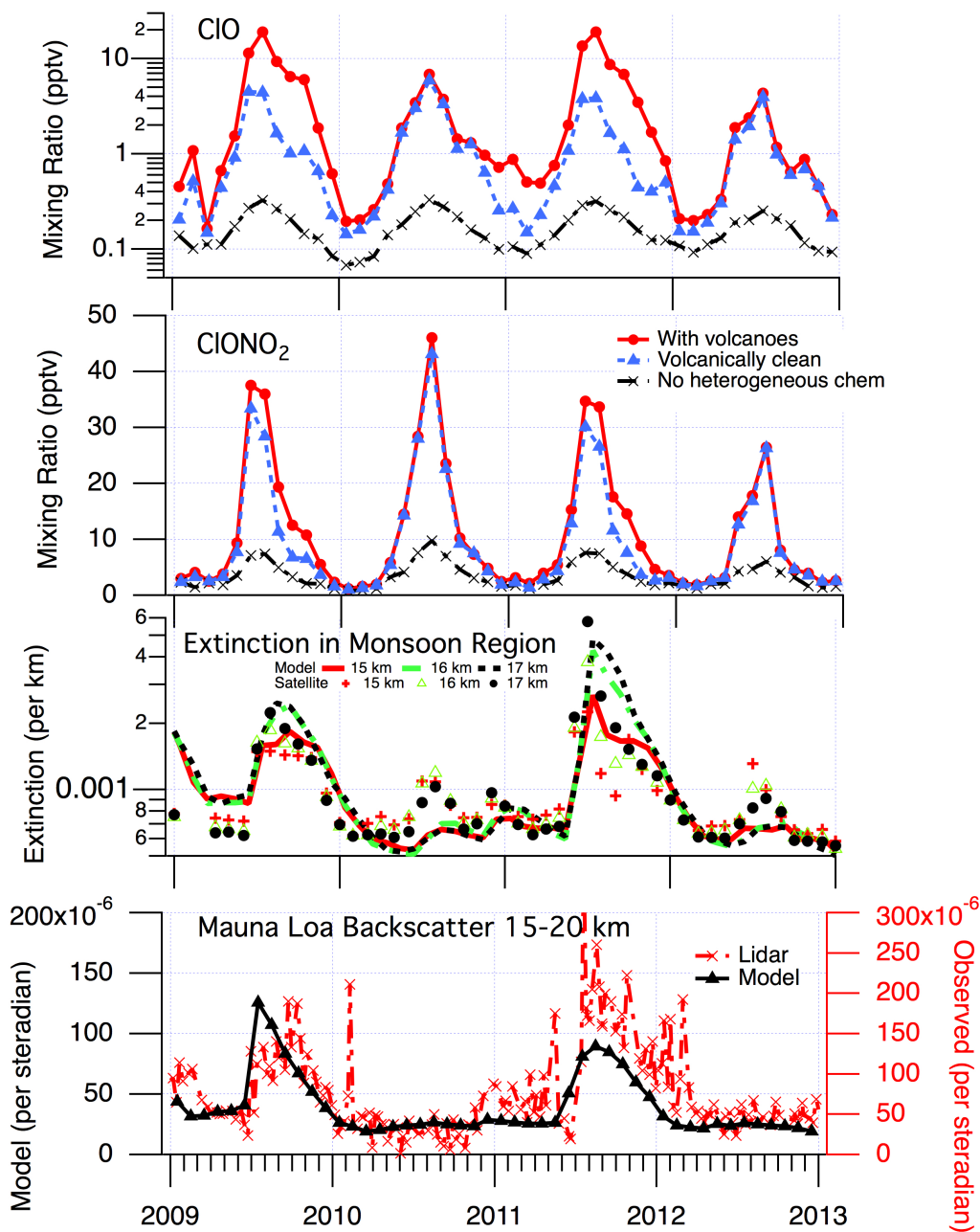
538



539

540 Figure 3. Zonally averaged ClONO₂ abundances (pptv) in July 2011 versus latitude and
 541 altitude in SD-WACCM model calculations with (top) and without (bottom) low-latitude
 542 heterogeneous chlorine chemistry, including volcanic inputs. The location of the
 543 meteorological tropopause has been indicated with a dashed green line, and the red box
 544 highlights the region discussed.

545



546

547 Figure 4. Model-calculated chemical constituents (pptv) averaged over the latitude band
 548 14-20°N versus month at 17 km, for simulations with and without volcanic inputs, and
 549 without low-latitude heterogeneous chlorine chemistry, for 2009-2012 for ClO (top), and
 550 ClONO₂ (second from top). The time series of extinction at 532 nm measured by

551 satellite lidar, averaged over the monsoon region (15-45°N, 5-105°E, adapted from
552 Figure 2 of Vernier et al., 2015), compared to the model values at 15, 16, and 17 km
553 (third from top). Aerosol backscatter integrated over 15-20 km (bottom) at Mauna Loa
554 (per steradian) from observations (right axis) and from the model, assuming an
555 extinction-to-backscatter conversion factor of 40 (left axis). Note change in scale of the
556 two y-axes in the bottom panel.

557

558

[Geophysical Research Letters]

Supporting Information for

Monsoon circulations and
tropical heterogeneous chlorine chemistry in the stratosphere

Susan Solomon¹, Doug Kinnison², Rolando R. Garcia², Justin Bandoro¹, Michael Mills²,
Catherine Wilka¹, Ryan R. Neely III^{3,4}, Anja Schmidt³, John Barnes⁵, Jean Paul
Vernier^{6,7}, Michael Höpfner⁸

¹Department of Earth, Atmospheric, and Planetary Sciences, Massachusetts Institute of Technology,
Cambridge, MA 02139

²Atmospheric Chemistry Observations and Modeling Laboratory, National Center for Atmospheric
Research, Boulder, CO 80307

³School of Earth and Environment, University of Leeds, Leeds, UK

⁴National Centre for Atmospheric Science, University of Leeds, Leeds, UK

⁵NOAA/Mauna Loa Observatory, Hilo, HI 96720

⁶NASA Langley Research Center, Hampton, VA

⁷Science Systems and Applications, Inc., Hampton, VA

⁸Institute of Meteorology and Climate Research, Karlsruhe Institute of Technology, Karlsruhe, Germany

Contents of this file

Figure S1, S2, and Table S1

This file contains two figures and one table of supporting information cited in the main
article.

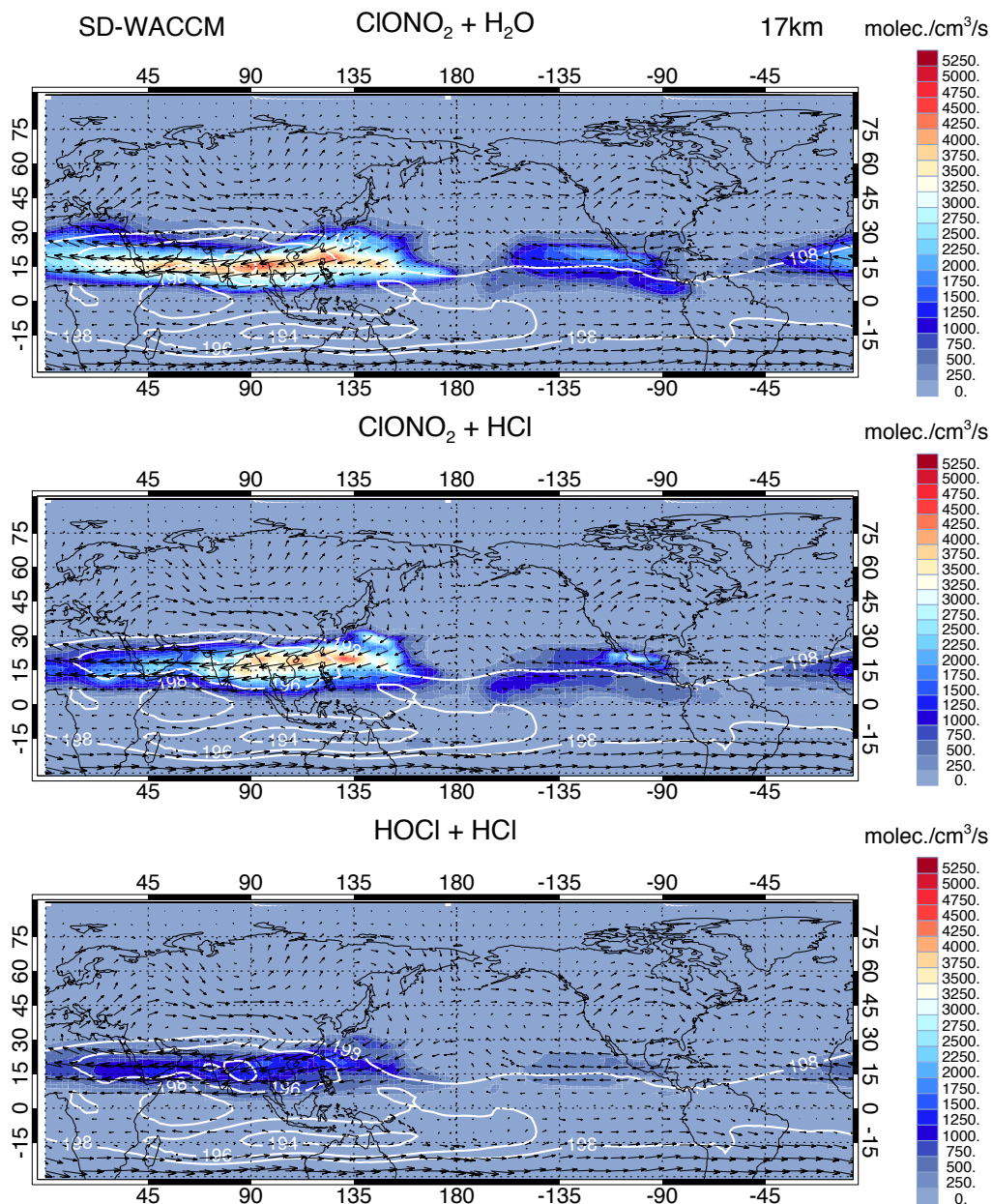


Figure S1. Calculated gross rates of key chlorine heterogeneous reactions for July 2011 at 17 km (molec cm⁻³ s⁻¹). The temperatures at this level are overlaid as white contours. The reactions shown are $\text{ClONO}_2 + \text{H}_2\text{O} \rightarrow \text{HNO}_3 + \text{HOCl}$ (top), $\text{ClONO}_2 + \text{HCl} \rightarrow \text{HNO}_3 + \text{Cl}_2$ (middle), and $\text{HOCl} + \text{HCl} \rightarrow \text{H}_2\text{O} + \text{Cl}_2$ (bottom). The $\text{ClONO}_2 + \text{H}_2\text{O}$ reaction exchanges one short-lived chlorine species for another (ClONO_2 becomes HOCl)

and does not represent net activation of chlorine. The $\text{ClONO}_2 + \text{HCl}$ and $\text{HOCl} + \text{HCl}$ reactions produce net activation of short-lived chlorine from the long-lived HCl reservoir.

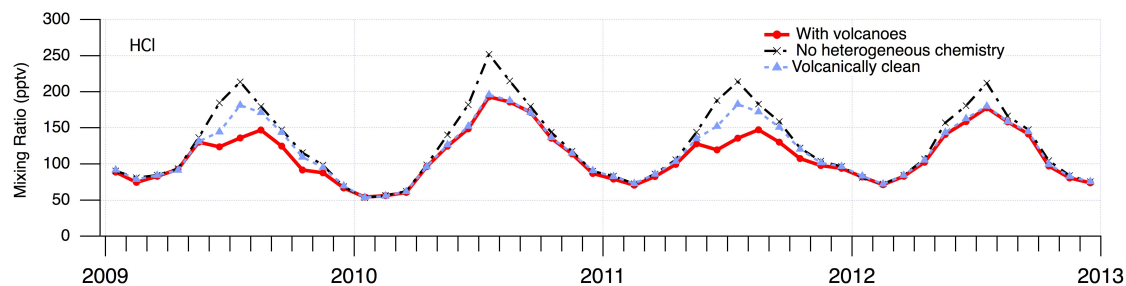


Figure S2. Model-calculated HCl mixing ratio (pptv) averaged over the latitude band from 14-20°N versus month at 17 km, for simulations with and without volcanic inputs, and without low-latitude heterogeneous chlorine chemistry, for 2009-2012; compare to Figure 4 of the main text.

Table S1. Reaction probabilities for the key $\text{ClONO}_2 + \text{HCl}$ reaction as a function of temperature for two different water vapor abundances at 85 hPa, representing typical conditions near the region of maximum activation around the monsoons as shown in Figure S1.

Temperature	$\text{ClONO}_2 + \text{HCl}$ (4.5 ppmv H_2O)	$\text{ClONO}_2 + \text{HCl}$ (5.5 ppmv H_2O)	$\text{HOCl} + \text{HCl}$ (4.5 ppmv)	$\text{HOCl} + \text{HCl}$ (5.5 ppmv)
194	0.11	0.28	0.022	0.042
196	0.014	0.039	0.0058	0.012
198	0.0023	0.0057	0.0016	0.0031
200	0.0005	0.0011	0.00045	0.00086